ISSN 1061-8309, Russian Journal of Nondestructive Testing, 2015, Vol. 51, No. 11, pp. 705–712. © Pleiades Publishing, Ltd., 2015.
Original Russian Text © A.N. Smirnov, V.I. Danilov, E.A. Ozhiganov, V.V. Gorbatenko, V.V. Murav'ev, 2015, published in Defektoskopiya, 2015, Vol. 51, No. 11, pp. 59–67.

ACOUSTIC METHODS

The Dependence of Local Deformations and Internal Stress Fields on Welding Technique for Grade VSt3sp Structural Steel: I. The Influence of Welding Technique on the Mechanical Characteristics and Acoustic Emission Parameters of Grade VSt3sp Steel

A. N. Smirnov[a]*, V. I. Danilov[b], E. A. Ozhiganov[a]***, V. V. Gorbatenko[b]****, and V. V. Murav'ev[c]*****

[a] *Kuzbass Center of Welding and Testing Co., pr. Lenina 33, Kemerovo, 650055 Russia*

[b] *Institute of Strength Physics and Materials Science, Siberian Division, Russian Academy of Sciences, Akademicheskii pr. 2/1, Tomsk, 634021 Russia*

[c] *Izhevsk State Technical University, ul. Studencheskaya 7, Izhevsk, 426069 Russia*

**e-mail: galvas.kem@gmail.ru*

***e-mail: dvi@ipms.tsc.ru*

****e-mail: zhidan84@mail.ru*

*****e-mail: gvv@ispms.tsc.ru*

******e-mail: vmuraviev@mail.ru*

Received December 25, 2014; in final form, March 24, 2015

Abstract—A staging analysis was carried out for deformation curves and the evolution of local deformation fields in defective and defect-free specimens of welded joints of grade VSt3sp steel that were made using manual arc and manual pulsed arc welding. Stages of elasticity, microplasticity, nucleation and motion of Chernov–Luder's bands, and parabolic deformation strengthening were considered. The parameters of acoustic-emission signals during tension of specimens with a welded seam were analyzed.

Keywords: internal stresses, local deformation fields, acoustic emission, welded joints, grade VSt3sp steel

DOI: 10.1134/S1061830915110066

INTRODUCTION

The refinement and increase in the reliability of base metal and welded joints that are in long-term operation under complex stressed conditions in corrosive media are important problem in many industries, including heat power generation, atomic, and gas-and-oil industries. In the context of developments for solving this problem in Russia, new techniques for welding, testing, and diagnosis, as well as new materials and facility have been developed and implemented [1–3]. However, more than 50% of all welded joints are performed using manual arc welding (MAW) because of its unique abilities for the execution of welding works under the most complex conditions and in out-of-the-way places [4]. Therefore, various techniques of manual pulsed arc welding (MPAW), which have been developed recently and have a large number of advantages in comparison with MAW, are of great interest [4, 5].

After the repair of erection work on engineering facilities of dangerous manufacturing objects there is a need to test their strength and hermeticity under loads that exceed operating ones, however, with low efficiency [6]. The stress-test technique is widely applied in foreign countries, its essence lies in the generation of internal pressure on tube walls that exceed the yield strength of steel because of the fact that critical and subcritical defects were revealed and residual stresses decrease.

The question of the influence of traditional tests and the stress-test technique on the physical–mechanical characteristics of materials, local fields of internal stresses, local deformations, and, as the consequence, on the working capacity of a facility, is still open.

The aim of the present research is an investigation of the influence of manual arc-welding and manual pulsed arc-welding techniques, as well as the influence on the degree of deformation and type of artificially induced defects on the acoustic emission (AE) signal parameters, mechanical characteristics, and the character of the local deformation field in welded joints that were made with grade VSt3sp steel (GOST (State Standard) 380–2005).

MATERIALS AND METHODS

The experiments were carried out using a tube that was 159 mm in diameter and 5 mm in thickness that was made of the most widespread grade VSt3sp structural carbon steel. The welding was performed using E50A electrodes: one half of the joints were made using MAW with a stationary arc and other were performed using MPAW with pulse-current modulation. The joint type was S17 (GOST 5264–80). To obtain artificial defects, we used graphite and broken glass, which were placed into the bottom run. Graphite and silicate nonmetallic inclusions were modeled using this method. Completed joints were machined with weld reinforcement relieving according to GOST 6996–66.

Mechanical tests and investigations of deformation fields were carried out using proportional plane specimens of the double blade type according to GOST 1497–84 with operating part sizes of $2.8 \times 6.0 \times 50.0$ mm. The welded seam was placed perpendicularly to the extension axis in the middle of the operating part of the specimen. The uniaxial tensile tests were performed using a Walter+Bai AG LFM-125 universal testing machine (Switzerland). The travel velocity of the movable catch was 0.2 mm/min, which corresponded to a deformation rate of 6.7×10^{-5} s^{-1} (quasistatic mode).

The point displacement fields on the operating specimen part were recorded during loading. To perform this operation the double-exposed speckle photography technique that was described in detail in [7] was used. The behavior of the deformation fronts on the yield plateau was studied using a digital variant of speckle photography [8].

Recording and analyzing AE signals in the specimens that were used for mechanical tests were not suitable because of the small sizes of the operating parts; therefore, plane specimens without heads were made with sizes of $5.0 \times 15.0 \times 200.0$ mm. Tests were carried out using a RM-50M tension testing machine. The average loading rate was 20 N/s. Apart from the usual tension to rupture, stepwise loading to various plastic deformation degrees of 1, 2, 3, and 5% was performed. After each of these tests we carried out a complex investigation with the analysis of the level of corresponding stresses. No less than five specimens were tested in every mode.

AE signals were recorded using an A-line 32D multichannel system (INTERUNIS Ltd.). The loading process was monitored using GT200 acoustic emission converters (AECs) with a transmission band of 130–200 kHz. The amplification over channels was 26 dB. The radar type is linear and the distance between AECs is 150 mm. AECs were mounted at the location of the machine capture on the rigid parts of specimens. We used Litol-24 as a contact material. The system was calibrated using an AE signal imitator (amplitude of 10 V, frequency of 1 Hz). It should be noted that to eliminate spurious signals of acoustic re-reflections (because of the small sizes of the specimens that were investigated) the DeadTime parameter[1] during the adjustment of the AE system was increased to 32 ms by programming.

RESULTS AND DISCUSSION

The first step presented the visual and ultrasonic inspection and the macroanalysis of welded joints. The welded joints with graphite and glass that were placed in the bottom run had defects in the form of chains of nonmetallic inclusions; cracks were not revealed.

The following step was mechanical testing of specimens that were made by various welding methods. Figure 1 shows the tensile diagram of the specimen that was made using manual arc welding. It is evident that microplasticity (deviation from the Hooke law) occurred beginning at $\varepsilon_e = 0.007$. This is expressed not only in the diagram bend, but in the occurrence of small stress jumps as well. At $\varepsilon_s = 0.016$ the diagram demonstrates sharp yield point $\sigma_Y = 338$ MPa and the origin of the yield plateau; however, the flow process on it is unstable and developed step-wise. With the attainment of $\varepsilon_f = 0.027$ the yield plateau ends and begins deformation strengthening of the parabolic type. Tensile strength $\sigma_b = 505$ MPa is attained at $\varepsilon_b = 0.155$. The rupture occurred through the base metal in the heat-affected area (HAA) of the weld.

Thus, the diagram can be divided into the following stage: an elastic site (Hook law is fulfilled); the microplasticity stage; the yield plateau (Chernov–Luder's deformation); the parabolic deformation

[1] This is the time after the termination of the AE pulse, during which the AE channel cannot record other AE pulses.

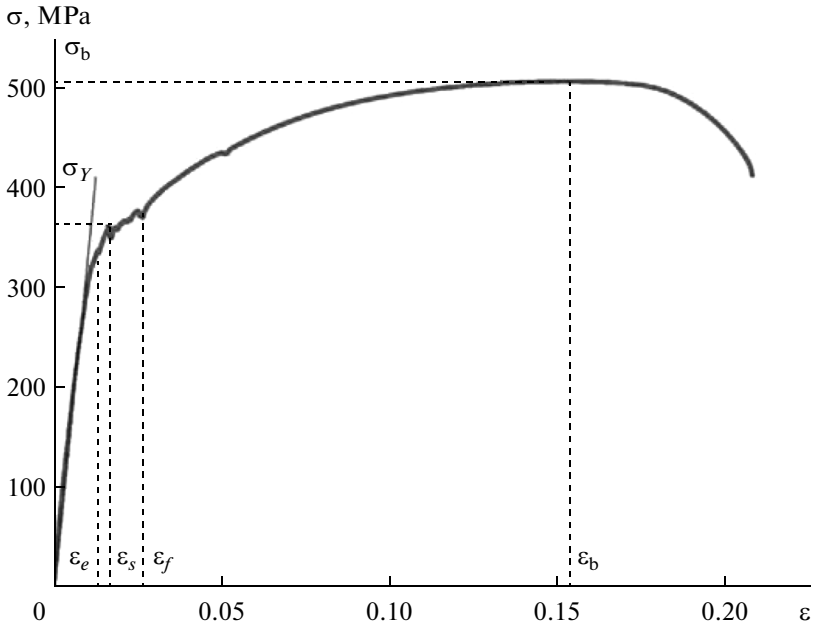

Fig. 1. The tensile diagram of the specimen of a welded joint that was made by MAW without artificial defects.

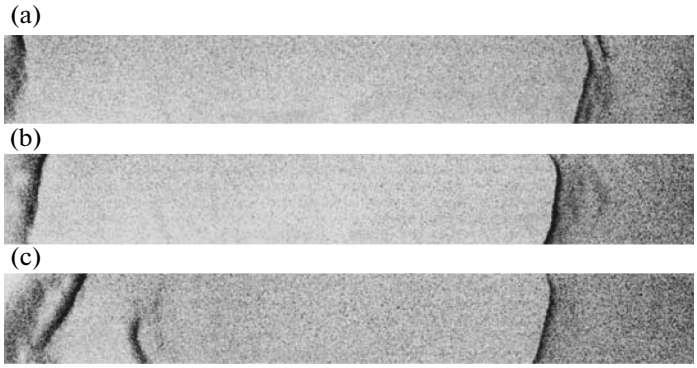

Fig. 2. The displacement of Chernov–Luder's bands on the yield plateau of the specimen with the welded seam that was made by MAW without defects. a–c, band locations at total deformations of 0.017, 0.022, and 0.027, respectively.

strengthening stage; loss of the macroscopic stability of the plastic flow; and the beginning of the formation of the rupture neck. The drooping site of the deformation curve corresponds to the localized deformation in the rupture neck.

Digital speckle photography revealed that at the yield plateau the displacement of the deformation front occurred, viz., Chernov–Luder bands over the operating part of the specimen (Fig. 2).

It should be noted that the described loading diagram for the investigated specimen is typical. Its overall stage and features were repeated on the qualitative level during tests of welded joint specimens that were made using both MAW and MPAW without artificial defects and with defects. The table gives the parameters of the deformation curves, which were averaged over five welded joint specimens that were performed using each of the mentioned methods.

Thus, we observed the microplasticity stage in a deformation range of (1.02–1.82) ± 0.25%, Chernov–Luder's deformation in a deformation range of (1.82–2.2) ± 0.25%, and parabolic strengthening to a deformation of 13.3 ± 1.0%. The observed quantities of the yield strength in a range of 327–377 MPa and a tensile strength of 498–507 MPa correspond to GOST 380–2005 for grade VSt3sp steel.

Tests of specimens without heads provided similar results (compare the data of the table and Fig. 3). Therefore, the measurement of AE signals during the deformation of such specimens must not distort the pattern of proceeding processes.

Strength parameters and deformation levels

Mode	ε_e, %	ε_s, %	ε_f, %	ε_b, %	σ_Y, MPa	σ_b, MPa
MAW	1.0	1.7	2.9	14.6	347	505
MPAW	0.7	1.5	2.6	12.1	377	507
MAW + defects	1.1	2.0	3.2	13.0	327	498
MPAW + defects	1.3	2.1	2.9	13.6	337	500

As is evident from the graphs (Fig. 3), when testing specimens that were made by various welding methods the deformation is observed in the first place under stresses of 250 MPa for defect specimens that were welded using MAW. The defect-free specimens that were performed by MPAW begin to deform under stresses of 335 MPa. The stress spread reached 85 MPa at the initial stage. However, the curves approach at a deformation above 2%; overall, investigated specimens (which were welded in various conditions) were ruptured within one stress range under loads of 460–500 MPa in the heat-affected area (HAA).

The specimen load changed the AE characteristics (Fig. 4). The presence of AE signals in the region of small total deformation (to 2%) can be explained by the fact that the nucleation and motion of Chernov–Luder's bands occur at this stage. According to some concepts [9, 10], the onset of the macroscopically uniform plastic deformation of a loaded object occurs in single microvolumes. These were single grains that are independent of one other in polycrystals. Next, grain groups occur in which the plastic deformation is correlated. These areas were the nuclei of Chernov–Luder's bands, in which the deformation is localized at every instant of time. The Chernov–Luder's band nucleus must "intergrow" through the overall cross section of the specimen; only then does the band begin to travel over the specimen. Often several bands occur (two in our case, see Fig. 2). In cases where the band nucleates, intergrows through the section of the specimen, and travels over the specimen, deformation processes occur only at the comparatively narrow front, which separates the deformed part from the deformation-free one.

The plastic deformation gradients at the front were quite large. AE sources were practically completely concentrated at these fronts. In [11] this was experimentally verified by the simultaneous registration of the front of the traveling band and the location of AE sources.

The abrupt change in the curve of the total AE with an increase in the load and a decrease in amplitude quantities (after 2% of deformation) were connected with the fact that traveling deformation fronts were absent at the parabolic strengthening stage. In accordance with the rule of the correspondence of types of localized deformation autowaves to deformation curve stages [12], during parabolic strengthening a stationary dissipative structure occurs as an equidistant system of plastic deformation sites in which the

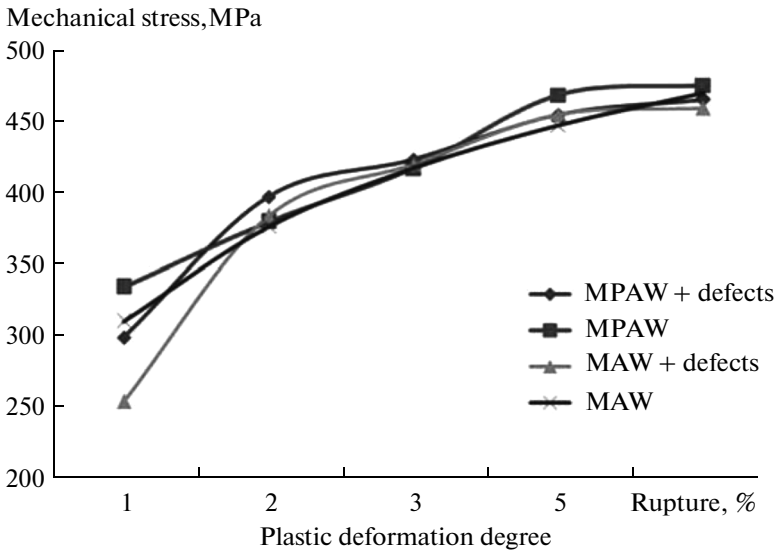

Fig. 3. Stresses that were applied to specimens of grade VSt3sp steel as a function of the degree of plastic deformation.

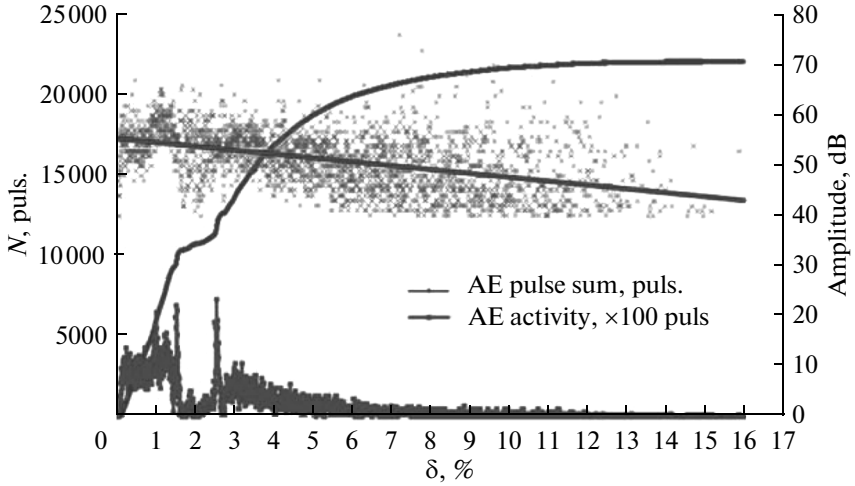

Fig. 4. The change in AE parameters with the deformation of the VSt3sp specimen that was made by MAW without artificial defects.

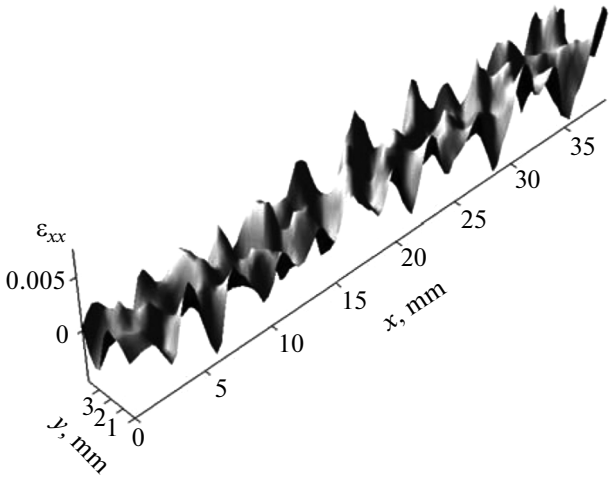

Fig. 5. The distribution of the local elongations ε_{xx} in the deformed specimen at the parabolic strengthening stage (MAW without defects, total deformation of 5.3%).

deformation amplitude is higher than in ambient areas (Fig. 5). At the same time, the deformation gradients at site interfaces were substantially lower than at traveling fronts on the yield plateau. The AE-pulse amplitudes decrease at the given stage in a natural manner. The total AE decreases as well; however, the pulse spread over the amplitudes increases.

The performed approximation of the amplitude distributions of AE pulses for small deformations (to 2%) shows the compliance with the nucleation and motion of Chernov–Luder bands and meets the strengthening of the parabolic deformation. In defect-free specimens (MAW) that were deformed to 2% we recorded low-amplitude pulses (55 dB); specimens that were welded by MPAW show a significantly higher amplitude (by 4 dB) (Fig. 6). Specimens with defects have equal amplitudes (57 dB).

With a total deformation above 2% the amplitude for defect-free specimens (MAW) attained 54 dB, i.e., it practically was the same as at a deformation to 2%. With a total deformation above 2% the highest amplitude (Fig. 7) is recorded for specimens that were welded by MPAW (57 dB). Specimens with defects show similar AE signal amplitudes (54–55 dB); however, the signal-amplitude dispersion is higher than for defective specimens that were deformed to 2%. This fact may indicate an increase in the number of various low-energy AE sources.

One of the significant characteristics of the AE technique for the understanding of processes that occurred in the object under investigation is the pulse source coordinates. There were two main methods

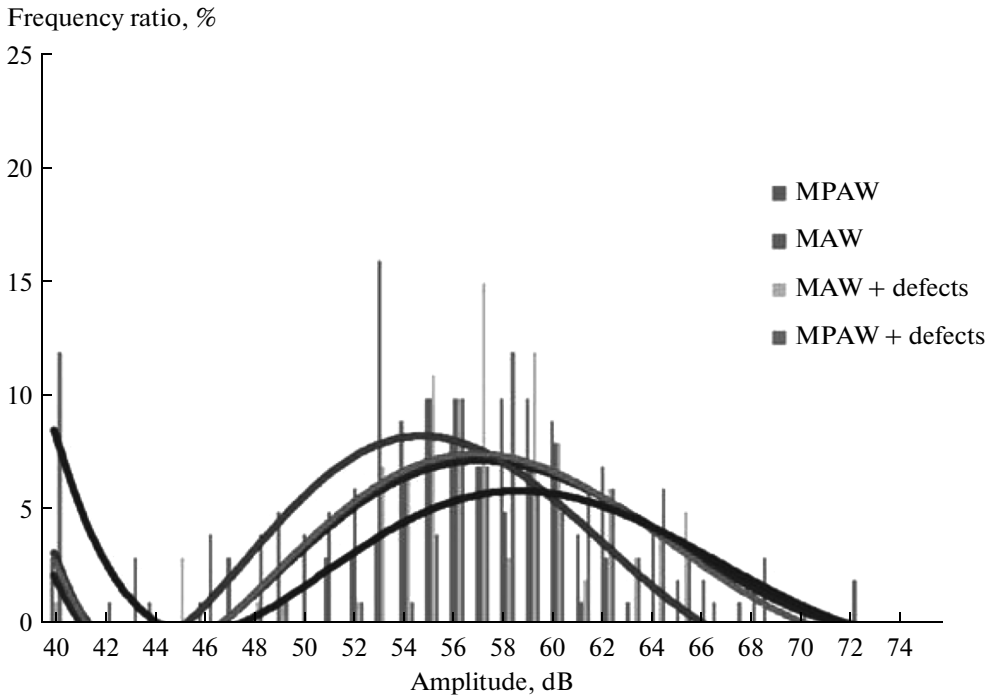

Fig. 6. An approximation of the AE-signal amplitude distributions during deformation to 2%.

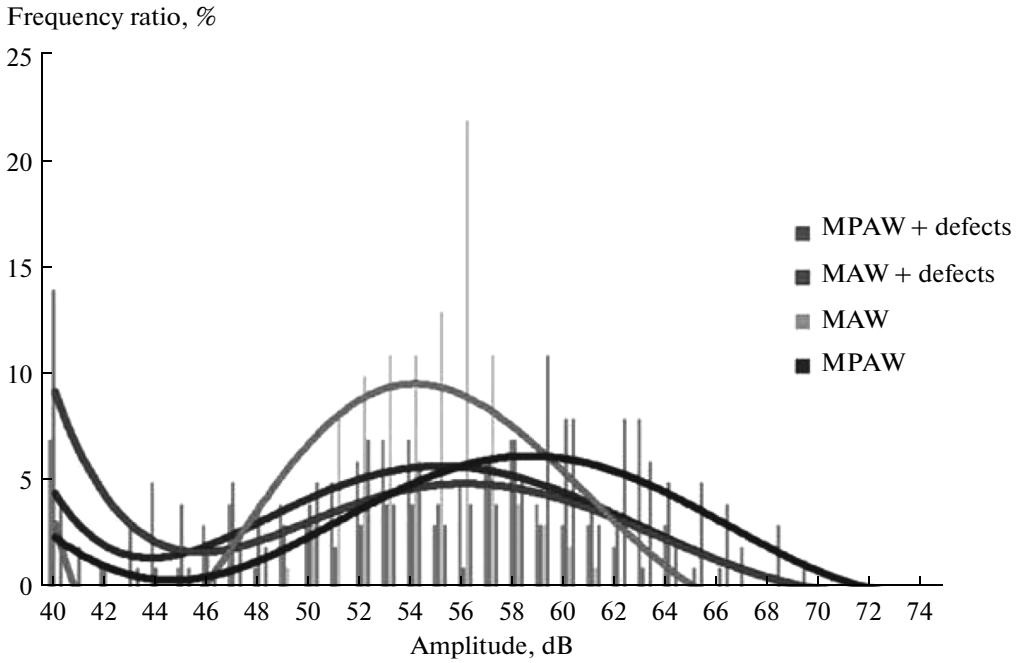

Fig. 7. An approximation of the AE signal-amplitude distributions at a deformation above 2%.

of AE-source localization: a temporal method, which is based on the time difference of the arrival (TDA) of a signal to AECs, and an amplitude method, which is based on the dependence of the acoustic wave attenuation on the distance between the AE source and the AECs [13–15]. For comparatively small and fine objects we performed localization by TDA, which made it possible to determine the AE-source coordinates most exactly.

In specimens that were made by MPAW (Fig. 8) with a change in the deformation degree the majority of AE signal sources were concentrated over specimen edges, about attaching points, and in the area of the

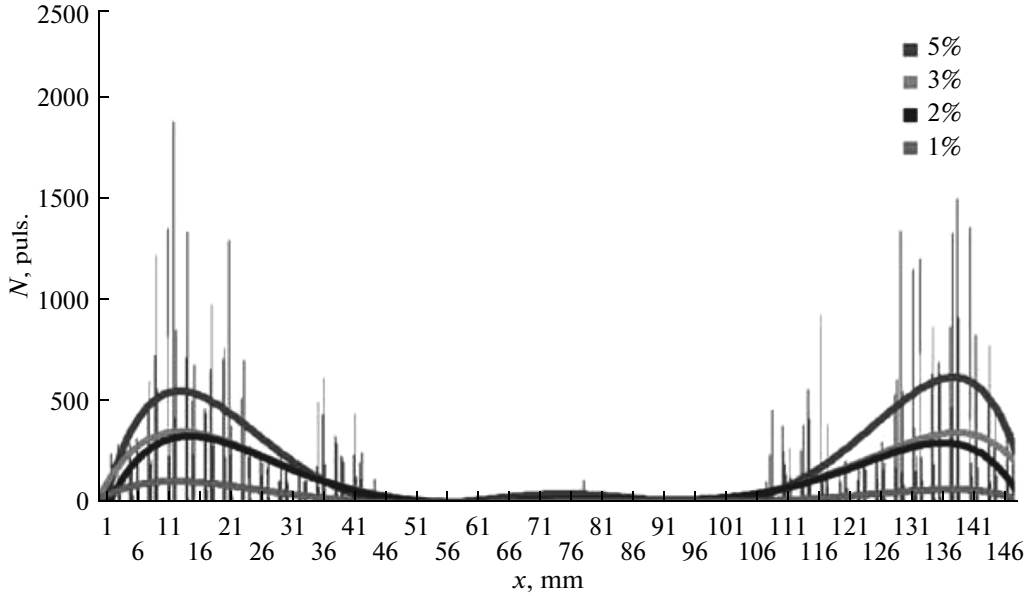

Fig. 8. An approximation of AE signal locations of VSt3sp specimens that was performed by MPAW with artificial defects upon changing the degree of deformation.

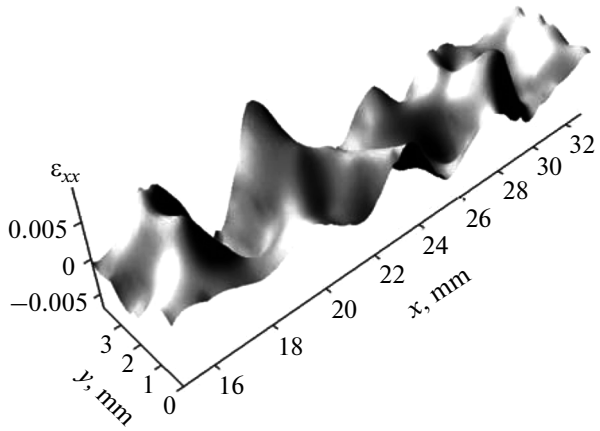

Fig. 9. The distribution of local elongations ε_{xx} in the deformed specimen at the parabolic strengthening stage (MPAW + defects, total deformation of 11.8%).

higher stress concentrations. When the load was increased the level of these signals increased. At the parabolic strengthening stage AE signals began to be revealed in the HAA, i.e., in the zone of the future rupture. This fact also affects the location deformation distributions.

From Fig. 9 it is evident that the maximum local elongations were observed in the area of the location of the welded seam at $x = 20–22$ mm. It should be noted that the number of AE signals at the location diagram is practically invariable in a deformation range from 2 to 5%, i.e., at transition from the Chernov–Luder's deformation to the parabolic strengthening stage.

CONCLUSIONS

(i) A staging analysis of deformation curves and the evolution of local deformation fields showed that for the overall investigated welded joints of grade VSt3sp steel (which were welded by MAW and MPAW) one can observe the microplasticity stage in a deformation range of (1.02–1.82) ± 0.25%, Chernov–Luder's deformation in a deformation range of (1.82–2.2) ± 0.25%, and parabolic strengthening to a deformation of 13.3 ± 1.0%. The observed quantities of the yield strength were in the range of 327–377 MPa; the tensile strength was in the range of 498–507 MP.

(ii) With small degrees of total deformation to 2% the microplasticity stage in defective specimens that were made by MAW began at the minimum load (stress on the order of 250 MPa) and in defect-free welded joints made by MPAW the microplasticity stage occurred under the maximum load (stress in the range of 335 MPa). With a transition to the parabolic deformation strengthening stage (a total deformations of from 2 to 5%) the difference decreased and the defective and defect-free specimens were deformed practically at the same stresses. Specimen rupture always occurred over the heat-affected area.

(iii) The average amplitudes of AE signals of defect-free specimens that were made by MAW and MPAW had an equal level of 54–55 and 58 dB with common deformations (to 2 and above 2%, respectively). Specimens that were made by MAW and MPAW with artificial defects had a decrease in the average amplitudes of AE signals to 54–55 dB with common deformations above 2% that were accompanied by a significant increase in the dispersion of the AE signal amplitude.

(iv) The zone of the outstanding specimen rupture was revealed both by TDA of AE signals and by patterns of local deformation distributions only at the parabolic deformation strengthening stage when the common deformation degree was higher than 3%.

(v) The influence of artificial defects (nonmetallic inclusions) within welded joints of grade VSt3sp steel, independently of the welding technique, occurs in the form of a decrease in the stress level at the onset of the microplasticity stage, a decrease in the average amplitudes of AE signals in this load range, and an increase in the dispersion of AE-signal amplitudes.

ACKNOWLEDGMENTS

This work was supported by the Russian Foundation for Basic Research (project no. 14-08-00299) and the State Program of the Ministry of Education and Science of the Russian Federation (project no. 3.751.2014/K) for the Izhevsk State Technical University for 2014–2016.

REFERENCES

1. Aleshin, N.P., Estimation of residual lifetime for welded structures, *Svarka i Diagnostika*, 2014, no. 1, pp. 41–47.
2. Smirnov, A.N., Uglov, A.L., and Erofeev, V.I., *Akusticheskii kontrol' oborudovaniya pri izgotovlenii i ekspluatatsii* (Acoustical Surveillance of Facility in Manufacture and Operation), Moscow: Nauka, 2009.
3. Semashko, N.A., Shport, V.I., Mar'in, B.N., et al., *Akusticheskaya emissiya v eksperimental'nom materialovedenii* (Acoustic Emission in Experimental Material Science), Semashko, N.A, Eds., Moscow: Mashinostroenie, 2002.
4. Knyaz'kov, V.L. and Knyaz'kov, A.F., *Povyshenie effektivnosti ruchnoi dugovoi svarki truboprovodov* (Enhancement of Efficiency in Manual Arc Welding of Pipelines), Kemerovo: Kuzbass State Technical University, 2008.
5. Aleshin, N.P., Gladkov, E.A., Kuznetsov, P.S., Brodyagin, V.N., Kopoteva, E.N., and Sholokhov, M.A., Impulsive technologies for drop-transfer control during MIG/MAG welding, *Svarka i diagnostika*, 2014, no. 3, pp. 43–47.
6. Zorin, A.E. and Kas'yanov, A.N., Fatigue crack life of tube steels and their welded joints after elastoplastic deformation, *Svar. Proizvod.*, 2009, no. 10, pp. 29–30.
7. Danilov, V.I., Zuev, L.B., Gorbatenko, V.V., Gonchikov, K.V., and Pavlichev, K.V., Application of speckle interferometry for investigation of plastic deformation localization, *Zavod. Lab.*, 2006, vol. 72, no. 12, pp. 40–45.
8. Zuev, L.B., Gorbatenko, V.V., and Pavlichev, K.V., Elaboration of speckle photography techniques for plastic flow analyses, *Meas. Sci. Technol.* 2010, vol. 21, no. 5, p. 054014.
9. Dudarev, E.F., *Mikroplasticheskaya deformatsiya i predel tekuchesti polikristallov* (Microplastic Deformation and Yield Strength of Polycrystals), Tomsk: Izd-vo Tomskogo Gosuniversiteta, 1988.
10. Pelleg, J., *Mechanical Properties of Materials,* Heidelberg, New York, London: Springer, 2013.
11. Nikitin, E.S., Semukhin, B.S., and Zuev, L.B., Localized plastic flow and space-time distribution of acoustic signal emission, *Pis'ma Zh. Tekh. Fiz.*, 2008, vol. 34, no. 15, pp. 70–74.
12. Zuev, L.B., Danilov, V.I., and Barannikova, S.A., *Fizika makrolokalizatsii plasticheskogo techeniya* (Physics of Macrolocalization of Plastic Flow), Novosibirsk: Nauka, 2008.
13. Stepanova, L.N., Murav'ev, V.V., Kruglov, V.M., Kabanov, S.I., Lebedev, E.Yu., Metelkin, N.G., and Kozyatnik, I.I., RF Patent 2240551, *Byull. Izobret.*, 2003, no. 32, p. 20.
14. Stepanova, L.N., Ivliev, V.V., Murav'ev, V.V., Tyrin, V.P., Kabanov, S.I., and Lebedev, E.Yu., RF Patent 2296320, *Byull. Izobret.*, 2007, no. 9, p. 16.
15. Stepanova, L.N., Ser'eznov, A.N., and Murav'ev, V.V., Relations of AE signal spectrum with fatigue crack development in metallic specimens, *Kontrol'. Diagnostika*, 1999, no. 2, pp. 5–8.

Translated by S. Ordzhonikidze